Disturbance Observer-Based Fault-Tolerant Control for Robotic Systems with Guaranteed Prescribed Performance

Haifeng Huang, *Student Member, IEEE*, Wei He, *Senior Member, IEEE*, Jiashu Li, Bin Xu and Chenguang Yang, *Senior Member, IEEE*, Weicun Zhang

***Abstract*—The actuator failure compensation control problem of robotic systems possessing dynamic uncertainties has been investigated in this paper. Control design against partial loss of effective (PLOE) and total loss of effective (TLOE) of the actuator are considered and described respectively, and a disturbance observer (DO) using neural networks is constructed to attenuate the influence of unknown disturbance. Regarding the prescribed error bounds as time-varying constraints, control design method based on barrier Lyapunov function (BLF) is used to strictly guarantee both the steady-state performance and the transient performance. Simulation study on a two-link planar manipulator verifies the effectiveness of the proposed controllers in dealing with the prescribed performance, the system uncertainties and the unknown actuator failure simultaneously. Implementation on a Baxter robot gives a experimental verification of our controller.**

***Index Terms*—Actuator failure compensation, neural networks, prescribed performance, disturbance observer, barrier Lyapunov function, Baxter.**

I. Introduction

Nowadays, our daily life is increasingly relying on and demanding for robots [1-11]. As failures have a high probability of leading to damage on the environment or even causing a security incident, robotic systems inevitably need to be equipped with the ability of fault-tolerance, especially for robots with long-term and frequent physical human-robot interaction. Actuator, as the workhorse in the control system, is one of the most vulnerable components to failure because of the implementation of long-term continuous task. From the perspective of the effectiveness of executing control commands, actuator failure can be generally divided into two typical types: PLOE and TLOE. In robot systems, PLOE type of failure means that performance degradation occurs to actuators at one or more robot joints, and TLOE type of failure, often causing more serious consequence than PLOE, means that actuators at one or more robot joints are completely out of control. Both of them pose significant hurdles to the task execution if not handled properly. Over the past years, many effective methods have been proposed against actuator failures for nonlinear systems [12-14]. Among all of these methods, the adaptive failure compensation control approach avoids the effect of fault diagnosis error and has been used more and more recently [15-34]. While for the actuator failure compensation control of robotic systems, only under-actuated control [35] or PLOE of actuator [36] have been considered, more generic problems associated with which such as the uncertainties, the disturbance and the TLOE type of actuator failure need to be further investigated.

For the system uncertainties, learning-based control has been proved to be a mature way to overcome them [37-54]. In this paper, neural learning-based control technique is used. In practice, disturbances are usually difficult or even impossible to be measured physically by sensors in robot systems. To attenuate the disturbances promptly, control design based on DO has been widely studied [55-59]. Dominated by the uncertainties, common DOs no longer suit since most of them use the system information. Then the DO technique combined with neural network has been proposed and used [60]. However, few literatures consider the unknown actuator failure which means that the actual control signal cannot be obtained. In this paper, radial basis function (RBF) neural networks are utilized in the construction of the DO to estimate the unknown system dynamics and the unknown actuator torque coefficient.

With the raising requirements of robotic control systems, the dynamic performance of the robot is gradually being emphasized, which is directly characterized by the response speed and accuracy requirement. So another important problem is the prescribed performance at both transient and steady states [61-64]. Traditional nonlinear adaptive control design ensures that the tracking error converges to the residual set with a small size depending on the parameters selection. Nevertheless, how to systematically choose the above controller parameters to satisfy the prescribed state error in advance remains an ongoing challenge. Switching adaptive control technique used in [65] and [66] is an effective way to ensure the prescribed error bounds. Another effective method to guarantee the steady-state behavior is regarding this issue as an output constraint problem and then using the BLF method to overcome it [67-70]. What is more difficult to guarantee is the prescribed transient performance, by which we mean that both the convergence rate and the overshoot should be limited. Error transformation technique has been widely used to deal

H. Huang, W. He, J. Li and W. Zhang are with the School of Automation and Electrical Engineering, University of Science and Technology Beijing, Beijing 100083, China, and also with the Institute of Artificial Intelligence, University of Science and Technology Beijing, Beijing 100083, China. (Email: weihe@ieee.org)

B. Xu is with the School of Automation, Northwestern Polytechnical University, Xian 710072, China.

C. Yang is with the Bristol Robotics Laboratory, University of the West of England, Bristol, BS16 1QY, UK.

This work was supported by the National Natural Science Foundation of China under Grant 61873298, Grant 61622308, Grant 61873206, and the Natural Science Foundation of Beijing Municipality under Grant 4172041.

with prescribed performance bounds problem [71-75]. This method is novel and practical to deal with the control precision problem, but the performance functions are required to be positive and decreasing. Motivated by [76, 77], we regard the prescribed error bounds as time-varying constraints, and then control design method based on BLF is used to guarantee the prescribed performance, which relaxes the above limitation.

In this paper, we focus on the accommodation for unknown actuator failures, system uncertainties, unknown external disturbance and prescribed performance in the meantime. The main contributions are listed as follows:

(I) The prescribed performance control problem of uncertain robotic systems against both PLOE and TLOE of actuators is investigated for the first time, and the proposed control method is verified on a real robot platform.

(II) Control design method based on asymmetrical time-varying BLF is used to strictly guarantee both the steady-state performance and the transient performance.

(III) A novel DO combined with RBF neural networks is constructed to attenuate the influence of the disturbance.

In what follows, the preliminaries and problem formulation are given in Section II. Section III is divided into two parts which successively shows the design process of the two controllers against two typical types of failure, respectively. Section IV shows the numeric simulation work. Section V describes the experiment setup and results. Lastly, Section VI gives the conclusion and future work.

II. Preliminaries and Problem Formulation

In joint space, the dynamics model of a rigid robot that does not account for actuator failures can be described as follows:

$$M(q)\ddot{q} + C(q,\dot{q})\dot{q} + G(q) = \tau(t) - d(t) \tag{1}$$

where $q \in \mathbb{R}^n$, $\tau \in \mathbb{R}^n$, $M(q) \in \mathbb{R}^{n\times n}$, $C(q,\dot{q}) \in \mathbb{R}^{n\times n}$, $G(q) \in \mathbb{R}^n$, $d(t) \in \mathbb{R}^n$ are the vector of joint variables, the control input torque, the inertia matrix, the Coriolis and centrifugal matrix, the gravitational force, the external disturbance, respectively.

Property 1: [77] The inertia matrix $M(q)$ is symmetric and positive definite, and $\frac{1}{2}\dot{M}(q) - C(q,\dot{q})$ is skew-symmetric.

Property 2: [77] $M^{-1}(q)$ exists and is also positive definite and bounded. i.e. $\exists 0 < \beta < \infty$, such that $0 < M^{-1}(q) < \beta I_{n\times n}$ where I denotes identity matrix.

Assumption 1: The external disturbance $d(t)$ is assumed to be continuous and bounded. i.e. $\exists \bar{d} > 0$, such that $\forall t > 0, d \le \bar{d}$

Remark 1: $|\ast|$ denotes taking the absolute values of all the elements in the vector $\ast$.

Remark 2: $\lambda_{\min}(\bullet)$ and $\lambda_{\max}(\bullet)$ are the minimum and maximum eigenvalues of matrix $\bullet$, respectively.

Generally speaking, the actual torques generated by the actuators are exactly the commanded torques of the controller, but situation changes when the actuator failures occur. The control objective is to ensure that the output q follows the desired trajectory q_d while guaranteeing prescribed performance as well as the boundness of all close-loop signals even when some inevitable actuator failures take place.

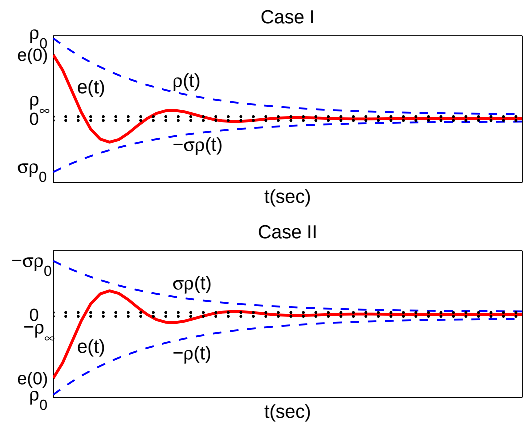

Fig. 1. Tracking error prescribed performance

When studying prescribed performance issue, it usually refers to three aspects: the minimum convergence rate, the maximum overshoot and the steady-state error bound. Motivated by [71, 72], a smooth positive performance function $\rho(t) = (\rho_0 - \rho_\infty)e^{-ht} + \rho_\infty$ is defined, where ρ_0, ρ_∞, h are positive constants to be designed. As shown in Fig. 1, $\rho(t)$ and $\sigma\rho(t)$ $(0 \le \sigma < 1)$ limit the tracking error behavior as long as the initial error is in the bound. Note that the decreasing rate of $\rho(t)$ represents the minimum allowable convergence rate, the steady-state error bounds are prescribed by ρ_∞ and $\sigma\rho_\infty$, and $\sigma\rho(0)$ reflects the overshoot of the error. Regarding the prescribed error bounds as time-varying constraints, Lyapunov direct method based on asymmetric time-varying BLFs is then used to cope with the prescribed performance problem.

III. Control Design and Stability Analysis

The actuator failure is divided into two types, PLOE and TLOE, and discussed in this section. The control design and the proof of system stability are mainly based on back-stepping technique and Lyapunov's direct method.

A. PLOE Type of Failure

When PLOE type of failure occurs, the dynamics model (1) is rewritten as

$$M(q)\ddot{q} + C(q,\dot{q})\dot{q} + G(q) = K_t\tau_c(t) - d(t) \tag{2}$$

where $\tau_c(t)$ denotes the commanded control input, the diagonal matrix $K_t = \mathrm{diag}[k_{t1}, k_{t2}, \cdots, k_{ti}, \cdots, k_{tn}]$ represents the actuator torque coefficient satisfying $0 < K_{ti} \le 1$. We define:

$$e = q - q_d = [e_1, e_2 \cdots e_n]^T \tag{3}$$

$$S = [S_1, S_1 \cdots S_n]^T = \dot{e} + \Lambda e \tag{4}$$

where e and S represent a tracking error and a generalized tracking error, $\Lambda = \mathrm{diag}[\Lambda_1, \Lambda_2 \cdots \Lambda_n]$ is a positive matrix to be designed. As mentioned above, the prescribe performance issue can be transformed into the time-varying constraints problem. In case I (or II), $\rho_i(t)$ (or $\sigma\rho_i(t)$) and $-\sigma\rho_i(t)$ (or $-\rho_i(t)$) represent the upper constraint and lower constraint of the tracking error e_i, respectively. For simplification, the upper constraint and lower constraint are expressed as $\overline{k}(t) = [\overline{k}_1, \overline{k}_2, \cdots, \overline{k}_i, \cdots, \overline{k}_n]^T$ and $\underline{k}(t) = [\underline{k}_1, \underline{k}_2, \cdots, \underline{k}_i, \cdots, \underline{k}_n]^T$. Introduce a BLF as follows:

$$\begin{aligned} V_1(t) = \sum_{i=1}^{n}[\frac{P(e_i)}{2}\ln\frac{\overline{k}_i^2(t)}{\overline{k}_i^2(t)-e_i^2(t)} \\ +\frac{1-P(e_i)}{2}\ln\frac{\underline{k}_i^2(t)}{\underline{k}_i^2(t)-e_i^2(t)}] \end{aligned} \tag{5}$$

where $P(e_i)$ is defined as

$$P(e_i) = \begin{cases} 0, & e_i \le 0 \\ 1, & e_i > 0 \quad i = 1, 2, 3, \cdots, n \end{cases} \tag{6}$$

Differentiating V_1 yields

$$\begin{aligned} \dot{V}_1 = \sum_{i=1}^{n}\big(\frac{P(e_i)e_i(t)}{\overline{k}_i^2(t)-e_i^2(t)}(S_i - \Lambda_i e_i(t) - e_i(t)\frac{\dot{\overline{k}}_i(t)}{\overline{k}_i(t)}) \\ +\frac{(1-P(e_i))e_i(t)}{\underline{k}_i^2(t)-e_i^2(t)}(S_i - \Lambda_i e_i(t) - e_i(t)\frac{\dot{\underline{k}}_i(t)}{\underline{k}_i(t)})\big) \end{aligned} \tag{7}$$

The diagonal matrix Λ is introduced as

$$\begin{aligned} \Lambda &= K_1 + \mu \\ &= \mathrm{diag}[k_{11}, k_{12}\cdots k_{1n}] + \mathrm{diag}[\mu_1, \mu_2\cdots\mu_n] \end{aligned} \tag{8}$$

where $K_1 \in \mathbb{R}^{n\times n}$ is a gain matrix and μ_i is defined as an upper bound of $\sqrt{(\frac{\dot{\overline{k}}_i(t)}{\overline{k}_i(t)})^2 + (\frac{\dot{\underline{k}}_i(t)}{\underline{k}_i(t)})^2}$, which can be easy found since $\overline{k}_i(t)$ and $\underline{k}_i(t)$ are the performance functions defined before. Here we give a simple proof to show the existence of the upper bound in the Case I:

$$\begin{aligned} \sqrt{(\frac{\dot{\overline{k}}_i(t)}{\overline{k}_i(t)})^2 + (\frac{\dot{\underline{k}}_i(t)}{\underline{k}_i(t)})^2} &= \sqrt{2}h(\frac{\rho_0-\rho_\infty}{\rho_0-\rho_\infty+\rho_\infty e^{lt}}) \\ &\le \sqrt{2}h \end{aligned} \tag{9}$$

Similar results can be proved for Case II. Combining (7) with (8), we have

$$\begin{aligned} \dot{V}_1 &\le -\sum_{i=1}^{n}k_{1i}e_i^2\big(\frac{P(e_i)}{\overline{k}_i^2(t)-e_i^2(t)} + \frac{1-P(e_i)}{\underline{k}_i^2(t)-e_i^2(t)}\big) \\ &\quad + \sum_{i=1}^{n}S_i\big(\frac{P(e_i)e_i(t)}{\overline{k}_i^2(t)-e_i^2(t)} + \frac{(1-P(e_i))e_i(t)}{\underline{k}_i^2(t)-e_i^2(t)}\big) \\ &\le -\sum_{i=1}^{n}k_{1i}e_i\xi_i + S^T\xi \end{aligned} \tag{10}$$

where the auxiliary variable $\xi = [\xi_1, \xi_2, \cdots, \xi_i, \cdots, \xi_n]^T$ is defined as

$$\xi_i = \frac{P(e_i)e_i(t)}{\overline{k}_i^2(t)-e_i^2(t)} + \frac{(1-P(e_i))e_i(t)}{\underline{k}_i^2(t)-e_i^2(t)} \tag{11}$$

Introduce a new Lyapunov function

$$V_2 = V_1 + \frac{1}{2}S^T M(q) S \tag{12}$$

Based on Property 1, we have

$$\begin{aligned} \dot{V}_2 &= \dot{V}_1 + \frac{1}{2}S^T\dot{M}(q)S + S^T M(q)\dot{S} \\ &= V_1 + \frac{1}{2}S^T\dot{M}(q)S + S^T M(q)\Lambda\dot{e} - S^T M(q)\ddot{q}_d \\ &\quad + S^T\big(K_t\tau_c - d(t) - G(q)\big) - S^T C(q,\dot{q})\dot{q} \\ &= \dot{V}_1 + S^T(K_t\tau_c - C(q,\dot{q})\dot{q}_d - G(q) - d(t) \\ &\quad - M(q)\ddot{q}_d + C(q,\dot{q})\Lambda e + M(q)\Lambda\dot{e}) \end{aligned} \tag{13}$$

Introduce a virtual controller α as

$$\begin{aligned} \alpha &= K_2 S + \xi - d(t) - C(q,\dot{q})\dot{q}_d - G(q) \\ &\quad - M(q)\ddot{q}_d + C(q,\dot{q})\Lambda e + M(q)\Lambda\dot{e} \end{aligned} \tag{14}$$

where $K_2 \in \mathbb{R}^{n\times n}$ is a positive diagonal matrix. Then, $\dot{V}_2$ can be reduced to

$$\dot{V}_2 = \dot{V}_1 + S^T(K_t\tau_c + \alpha - K_2 S - \xi) \tag{15}$$

Define $B = K_t^{-1} = [b_1, b_2, \cdots, b_i, \cdots, b_n]$ and the model-based fault-tolerant control law is proposed as

$$\begin{cases} \tau_c = -\hat{B}\alpha \\ \dot{\hat{b}}_i = S\alpha_i - \gamma_i\hat{b}_i, i = 1, 2, \cdots, n \end{cases} \tag{16}$$

where γ_i is a positive adjustable parameter, $\hat{B}$ and $\hat{b}$ are the approximations of B and b. Define $\tilde{b}_i = \hat{b}_i - b_i$, then consider a new Lyapunov function

$$V_3 = V_2 + \frac{1}{2}\sum_{i=1}^{n}\tilde{b}_i^T K_{ti}\tilde{b}_i \tag{17}$$

Differentiating V_3 yields

$$\begin{aligned} \dot{V}_3 =& \dot{V}_2 + \sum_{i=1}^{n}\tilde{b}_i^T K_{ti}S\alpha_i - \sum_{i=1}^{n}\tilde{b}_i^T K_{ti}\hat{b}_i \\ \le& \sum_{i=1}^{n}-k_{1i}e_i\xi_i + S^T(-K_t\hat{B}\alpha + \alpha - K_2 S) \\ &+ \sum_{i=1}^{n}\tilde{b}_i^T K_{ti}S\alpha_i - \sum_{i=1}^{n}\gamma_i\tilde{b}_i^T K_{ti}\hat{b}_i \end{aligned} \tag{18}$$

Combined with $-S^T K_t\hat{B}\alpha + S^T\alpha + \sum_{i=1}^{n}\tilde{b}_i^T K_{ti}S\alpha_i = 0$, we have

$$\dot{V}_3 \le -S^T K_2 S - \sum_{i=1}^{n}k_{1i}e_i\xi_i - \sum_{i=1}^{n}\gamma_i\tilde{b}_i^T K_{ti}\hat{b}_i \tag{19}$$

Applying Young's inequality, we have

$$\begin{aligned} -\tilde{b}_i^T K_{ti}\hat{b}_i &= -\tilde{b}_i^T K_{ti}\tilde{b}_i - \tilde{b}_i^T K_{ti}b_i \\ &\le -\tilde{b}_i^T K_{ti}\tilde{b}_i + \frac{1}{2}\tilde{b}_i^T K_{ti}\tilde{b}_i + \frac{1}{2}b_i^T K_{ti}b_i \\ &\le -\frac{1}{2}\tilde{b}_i^T K_{ti}\tilde{b}_i + \frac{1}{2}b_i^T K_{ti}b_i \end{aligned} \tag{20}$$

Plugging (20) into (19) yields

$$\dot{V}_3 \le -c_1 V_3 + c_2 \tag{21}$$

where c_1 and c_2 are two positive constant given as

$$c_1 = \min_{i=1,2\cdots n}(2\lambda_{\min}(K_1), \frac{2\lambda_{\min}(K_2)}{\lambda_{\max}(M(q))}, \gamma_i) \tag{22}$$

$$c_2 = \sum_{i=1}^{n} \frac{\gamma_i}{2} b_i^T K_{ti} b_i \tag{23}$$

The aforementioned controller is built on the premise that the dynamics information can be obtained, but the dynamics parameters are sometimes unmeasured or varied in robotic systems. In addition, the external disturbance is usually unknown and cannot be accurately measured by sensors. To solve these problems, learning control based on neural networks is employed, and a nonlinear DO is constructed. The uncertain continuous vector functions are estimated by two RBF neural networks as follows:

$$\begin{aligned} W^{*T}N(Z) =& -C(q,\dot{q})\dot{q}_d - M(q)\ddot{q}_d + C(q,\dot{q})\Lambda e \\ & - G(q) + M(q)\Lambda\dot{e} + \epsilon(Z) \end{aligned} \tag{24}$$

$$W_d^{*T}N_d(Z_d) = K_t\tau_c - C(q,\dot{q})\dot{q} + \epsilon_d(Z_d) - G(q) \tag{25}$$

where $Z = [q^T, \dot{q}^T, S^T]$ and $Z_d = [q^T, \dot{q}^T, \tau_c^T]$ are the RBF neural networks inputs , $N(Z) = [N_1(Z), N_2(Z) \cdots N_l(Z)]^T$ and $N_d(Z_d) = [N_{d1}(Z_d), N_{d2}(Z_d), \cdots, N_{dl}(Z_d)]^T$ are the regressor vectors with $N_i(Z)$ and $N_{di}(Z_d)$ being the Gaussian radial basis functions, $N_d(Z_d)$ satisfies $\parallel N_d(Z_d) \parallel \leq n_d$ with n_d being an unknown positive constant, l is the neural networks node number, $W^* = [W_1^*, W_2^*, \cdots, W_n^*]$ and $W_d^* = [W_{d1}^*, W_{d2}^*, \cdots, W_{dn}^*]$ are the weights of the two neural networks, $\epsilon(Z)$ and $\epsilon_d(Z_d)$ are the neural networks approximation errors satisfying $\mid \epsilon(Z) \mid \leq \bar{\epsilon}(Z)$ and $\mid \epsilon_d(Z_d) \mid \leq \bar{\epsilon}_d(Z_d)$. The weight adaption laws of the neural networks are set as

$$\dot{\hat{W}}_i = -\Gamma_i \left(N_i(Z)S_i + \sigma_i \hat{W}_i \right), i = 1, 2, \cdots, n \tag{26}$$

$$\dot{\hat{W}}_{di} = -\Gamma_{di} \left(N_{di}(Z_d)\hat{d}_i + \sigma_{di}\hat{W}_{di} \right), i = 1, 2, \cdots, n \tag{27}$$

where Γ_i and Γ_{di} are the constant gain matrixes, $\hat{d}$ is the approximation value of the disturbance, $\hat{W}$ and $\hat{W}_d$ are the estimations of the two weight vectors, σ_i and σ_{di} are small constants to avoid the drift of the $W^{*T}N(Z)$ and $W_d^{*T}N_d(Z_d)$, respectively. Introducing an auxiliary variable $\hat{z}$, the DO is constructed as

$$\begin{cases} \hat{d} = \hat{z} + k_d\dot{q} \\ \dot{\hat{z}} = -k_a\hat{z} - k_a \left(\hat{W}_d^T N_d(Z_d) + k_d\dot{q} \right) \end{cases} \tag{28}$$

where $k_a \in \mathbb{R}^{n\times n}$ and $k_d \in \mathbb{R}^{n\times n}$ are two diagonal matrixes satisfying $k_a \geq \beta k_d \geq k_d M^{-1}(q) > 0$. Then, $\dot{\hat{d}}$ becames

$$\begin{aligned} \dot{\hat{d}} =& -k_a(-k_d\dot{q} + \hat{d}) - k_a \left(\hat{W}_d^T N_d(Z_d) + k_d\dot{q} \right) \\ & + k_d M^{-1}(q) \left(K_t\tau_c - C(q,\dot{q})\dot{q} - G(q) - d \right) \\ =& -k_a\hat{d} - k_d M^{-1}(q) d - k_a\hat{W}_d^T N_d(Z_d) \\ & + k_d M^{-1}(q)\hat{W}_d^T N_d(Z_d) \end{aligned} \tag{29}$$

Applying Young's inequality we conclude that

$$\begin{aligned} \hat{d}^T\dot{\hat{d}} \leq& -\hat{d}^T k_a\hat{d} - \hat{d}^T k_d M^{-1}(q) d + |\hat{d}^T k_a \hat{W}_d^T N_d(Z_d)| \\ \leq& -\hat{d}^T k_a\hat{d} + \frac{1}{2}\hat{d}^T k_d M^{-1}(q)\hat{d} + \frac{1}{2}\bar{d}^T k_d M^{-1}(q)\bar{d} \\ & + \frac{1}{2}\bar{\epsilon}_d^T k_a^2 \bar{\epsilon}_d + \frac{1}{2}\hat{d}^T\hat{d} + \frac{1}{2}\hat{d}^T\hat{d} + \frac{1}{2} n_d W_d^{*T} k_a^2 W_d^* \\ \leq& -\hat{d}^T \big(k_a - \frac{1}{2}\beta k_d - I \big)\hat{d} + \frac{1}{2}\bar{d}^T \beta k_d \bar{d} \\ & + \frac{1}{2}\bar{\epsilon}_d^T(Z_d) k_a^2 \bar{\epsilon}_d(Z_d) + \frac{1}{2} n_d \parallel k_a W_d^* \parallel^2 \end{aligned} \tag{30}$$

The virtual control α is rewritten as

$$\alpha = K_2 S + \hat{W}^T N(Z) + \xi - \hat{d} \tag{31}$$

Consider an overall Lyapunov function

$$V_4 = V_3 + \frac{1}{2}\sum_{i=1}^{n} (\tilde{W}_i^T \Gamma_i^{-1} \tilde{W}_i + \tilde{W}_{di}^T \Gamma_{di}^{-1} \tilde{W}_{di}) + \frac{1}{2}\hat{d}^T\hat{d} \tag{32}$$

where $\tilde{W}_i = \hat{W}_i - W_i^*$ and $\tilde{W}_{di} = \hat{W}_{di} - W_{di}^*$ are the neural networks approximation errors, $\tilde{d} = \hat{d} - d$ is the DO error. Applying Young's inequality, the derivative of V_4 can be written as

$$\begin{aligned} \dot{V}_4 \leq& -\sum_{i=1}^{n} k_{1i} e_i \xi_i - S^T(K_2 - \frac{3}{2}I)S - \sum_{i=1}^{n} \frac{\gamma_i}{2}\tilde{b}_i^T K_{ti}\tilde{b}_i \\ & - \sum_{i=1}^{n} \frac{1}{2}\tilde{W}_i^T \sigma_i \tilde{W}_i - \hat{d}^T(k_a - 2I - \frac{1}{2}\beta k_d)\hat{d} \\ & - \sum_{i=1}^{n} \frac{1}{2}\tilde{W}_{di}^T \sigma_{di}\tilde{W}_{di} + \sum_{i=1}^{n} \frac{1}{2} W_i^{*T}\sigma_i W_i^* \\ & + \frac{1}{2}\bar{d}^T(I + \beta k_d)\bar{d} + \frac{1}{2}\bar{\epsilon}^T(Z)\bar{\epsilon}(Z) + \frac{1}{2}\bar{\epsilon}_d^T(Z_d)\Big(I \\ & + k_a^2\Big)\bar{\epsilon}_d(Z_d) + \frac{1}{2}\sum_{i=1}^{n} W_{di}^{*T}\sigma_{di}W_{di}^* \\ & + \sum_{i=1}^{n} \frac{\gamma_i}{2} b_i^T K_{ti} b_i + \frac{1}{2} n_d \parallel k_a W_d^* \parallel^2 \\ \leq& -c_3 V_4 + c_4 \end{aligned} \tag{33}$$

where c_3 and c_4 are two positive constants given as

$$\begin{aligned} c_3 =& \min_{i=1,2\cdots n} \Big(2\lambda_{\min}(K_1), \frac{2\lambda_{\min}(K_2 - \frac{3}{2}I)}{\lambda_{\max}(M(q))}, 2\lambda_{\min}(k_a \\ & - 2I - \frac{1}{2}\beta k_d), \gamma_i, \frac{\sigma_i}{\lambda_{\max}(\Gamma_i^{-1})}, \frac{\sigma_{di}}{\lambda_{\max}(\Gamma_{di}^{-1})} \Big) \end{aligned} \tag{34}$$

$$\begin{aligned} c_4 =& \sum_{i=1}^{n} \frac{1}{2} W_i^{*T}\sigma_i W_i^* + \frac{1}{2}\bar{d}^T(I + \beta k_d)\bar{d} + \frac{1}{2}\bar{\epsilon}^T(Z)\bar{\epsilon}(Z) \\ & + \frac{1}{2}\bar{\epsilon}_d^T(Z_d)(I + k_a^2)\bar{\epsilon}_d(Z_d) + \sum_{i=1}^{n} \frac{1}{2} W_{di}^{*T}\sigma_{di}W_{di}^* \\ & + \frac{1}{2} n_d \parallel k_a W_d^* \parallel^2 + \sum_{i=1}^{n} \frac{\gamma_i}{2} b_i^T K_{ti} b_i \end{aligned} \tag{35}$$

To ensure $c_3 > 0$, the gain matrix K_2, k_a and k_d are chosen to satisfy

$$\lambda_{\min}(K_2 - \frac{3}{2}I) > 0, \lambda_{\min}(k_a - 2I - \frac{1}{2}\beta k_d) > 0 \quad (36)$$

Multiplying both sides by $e^{c_3 t}$ in (33), and applying the integration over $[0, t]$, we have

$$\begin{aligned} V_4(t) \leq &(V_4(0) - \frac{c_4}{c_3})e^{-c_3 t} + \frac{c_4}{c_3} \\ \leq &V_4(0) + \frac{c_4}{c_3} \end{aligned} \quad (37)$$

Define $E = 2(V_4(0) + c_4/c_3)$, then the following inequalities hold:

$$\sqrt{1-e^{-E}}\underline{k}_i \leq e_i \leq \sqrt{1-e^{-E}}\overline{k}_i, ||\hat{d}|| \leq \sqrt{E} \quad (38)$$

$$||S|| \leq \sqrt{E/\lambda_{\min}(M(q))}, ||\tilde{b}_i|| \leq \sqrt{E/\lambda_{\min}(K_t^{-1})} \quad (39)$$

$$||\tilde{W}_i|| \leq \sqrt{E/\lambda_{\min}(\Gamma_i^{-1})}, ||\tilde{W}_{di}|| \leq \sqrt{E/\lambda_{\min}(\Gamma_{di}^{-1})} \quad (40)$$

Note that $E > 0$ and $\underline{k}_i < 0 < \overline{k}_i$, $\underline{k}_i < \sqrt{1-e^{-E}}\underline{k}_i \leq e_i \leq \sqrt{1-e^{-E}}\overline{k}_i < \overline{k}_i$ can be easily derived. Thus we can guarantee the tracking error within the prescribed bounds. From above, we know that $e, S, \hat{d}, \tilde{b}_i, \tilde{W}_i$ are bounded. Owing to the assumption 1 and the definition $\tilde{d} = \hat{d} - d$, the DO error is bounded. Because of the definition of S, we can know that $\dot{e}$ is bounded. Based on the boundness of $S, \tilde{W}_i, W_i, \hat{d}$ and in terms of $\alpha = K_2 S + \hat{W}^T N(Z) + \xi - \hat{d}$, α is bounded. Therefor, all signals in the closed-loop system are bounded.

Remark 3: According to the definition of E, if we set the c_3 relatively large, $\sqrt{1-e^{-E}}\underline{k}_i$ and $\sqrt{1-e^{-E}}\overline{k}_i$ will be smaller. Thus the tracking error can be guaranteed within a small neighborhood around zero by appropriately choosing design parameters.

Theorem 1: For the robotic system considering the PLOE of actuators (2), with bounded initial conditions, semi-global uniform boundedness (SGUB) stability is obtained under the control law (16) with the DO constructed as (28) and α designed as (31). The prescribed performance of the tracking error is guaranteed, namely $\forall t > 0$, $\underline{k}_i(t) < e_i(t) < \overline{k}_i(t)$.

B. TLOE Type of Failure

Different from PLOE, when TLOE type of failure occurs at some joint, these actuator outputs will be stuck at some unknown values and totally out of control. Considering that these values can even be zero, redundant control method is used to solve this problem, which provides greater flexibility in robotic systems [78]. In the presence of TLOE type of failure, the dynamics (1) can be rewritten as

$$\begin{cases} M(q)\ddot{q} + C(q,\dot{q})\dot{q} + G(q) = \tau_{tot}(t) = \tau_1(t) + \tau_2(t) \\ \tau_1(t) = \rho_1\tau_{c1}(t) + \bar{\tau}_{c1}(t) \\ \tau_2(t) = \rho_2\tau_{c2}(t) + \bar{\tau}_{c2}(t) \end{cases} \quad (41)$$

where $\rho_1, \rho_2 \in \mathbb{R}^{n\times n}$ are two diagonal matrixes denoting the actuator efficiency factors, $\tau_{tot}(t), \tau_1(t), \tau_2(t) \in \mathbb{R}^n$ are the actual control inputs, $\tau_{c1}(t), \tau_{c2}(t) \in \mathbb{R}^n$ are the commanded inputs of the control law, $\bar{\tau}_{c1}(t), \bar{\tau}_{c2}(t) \in \mathbb{R}^n$ are the unknown constant vectors denoting the stuck positions of the actuators. It is assumed that for anyone joint, the two redundant actuators cannot lose control at the same time.

Remark 4: We have $\rho_i\bar{\tau}_{ci} = 0, i = 1, 2$, which means that PLOE and TLOE types of failure can never occur to one actuator at the same time.

We first consider that $\rho_1, \rho_2, \bar{\tau}_{c1}, \bar{\tau}_{c2}$ are all known, the control law is given as

$$\tau_{c1} = -K_{11}\alpha - K_{12}, \tau_{c2} = -K_{21}\alpha - K_{22} \quad (42)$$

where $K_{11}, K_{12}, K_{21}, K_{22} \in \mathbb{R}^{n\times n}$ are diagonal matrixes that can be calculated by

$$\begin{cases} \rho_1 K_{11} + \rho_2 K_{21} = I \\ \rho_1 K_{12} + \rho_2 K_{22} = \bar{\tau}_{c1} + \bar{\tau}_{c2} \end{cases} \quad (43)$$

When we know all information of the system, including the dynamics, the disturbance and the failures, we rewritten $\dot{V}_2$ as

$$\begin{aligned} \dot{V}_2 = &\dot{V}_1 + S^T(\tau_1(t) + \tau_2(t) - K_2 S - \xi + \alpha) \\ = &\dot{V}_1 + S^T(-\rho_1 K_{11}\alpha - \rho_2 K_{21}\alpha - \rho_1 K_{12} \\ &- \rho_2 K_{22} + \bar{\tau}_{c1} + \bar{\tau}_{c2} + \alpha - K_2 S - \xi) \\ = &\dot{V}_1 - S^T K_2 S - S^T \xi \end{aligned} \quad (44)$$

Since $\rho_1, \rho_2, \bar{\tau}_{c1}, \bar{\tau}_{c2}$ are all unknown, $K_{11}, K_{12}, K_{21}, K_{22}$ cannot be obtained. To overcome this challenge, the adaptive parameter adjustment technique is employed, the feasibility of which is guaranteed by the existence of the solution of (43). The adaptive laws are designed as follows:

$$\dot{\hat{K}}_{i1} = S\alpha^T - \gamma_i\hat{K}_{i1}, \dot{\hat{K}}_{i2} = S - \gamma_i\hat{K}_{i2} \quad (45)$$

where $\hat{K}_{ij}(i = 1, 2; j = 1, 2)$ is the estimation of K_{ij}. Hence, the control law is rewritten as

$$\tau_{c1} = -\hat{K}_{11}\alpha - \hat{K}_{12}, \tau_{c2} = -\hat{K}_{21}\alpha - \hat{K}_{22} \quad (46)$$

Different from the above controller against PLOE type of failure, the neural networks used to construct the DO should be changed. (25) is rewritten as

$$\begin{aligned} W_D^{*T} N_D(Z_D) = &\rho_1\tau_{c1}(t) + \bar{\tau}_{c1}(t) + \rho_2\tau_{c2}(t) - G(q) \\ &- C(q,\dot{q})\dot{q} + \epsilon_D(Z_D) + \bar{\tau}_{c2}(t) \end{aligned} \quad (47)$$

where $Z_D = [q^T, \dot{q}^T, \tau_{c1}^T, \tau_{c2}^T]$ is the RBF neural networks input, $N_D(Z_D) = [N_{D1}(Z_D), N_{D2}(Z_D), \cdots, N_{Dl'}(Z_D)]^T$ is the regressor vector with $N_{Di}(Z_D)$ being the Gaussian radial basis function, $N_D(Z_D)$ satisfies $\parallel N_D(Z_D) \parallel \leq n_D$ with n_D being an unknown positive constant, l' is the node number, $\epsilon_D(Z_D)$ is the approximation error satisfying $\parallel \epsilon_D(Z_D) \parallel \leq \bar{\epsilon}_D(Z_D)$. The weights adaption law is given as

$$\dot{\hat{W}}_{Di} = -\Gamma_{Di}(N_{Di}(Z_D)\hat{d} + \sigma_{Di}\hat{W}_{Di}) \quad (48)$$

Similar to (28), the DO is constructed as

$$\begin{cases} \hat{d} = \hat{z} + k_d\dot{q} \\ \dot{\hat{z}} = -k_a\hat{z} - k_a\left(\hat{W}_D N_D(Z_D) + k_d\dot{q}\right) \end{cases} \quad (49)$$

Consider a new overall Lyapunov function

$$\begin{aligned} V_5 = V_2 + \sum_{i=1}^{n} \frac{1}{2}\tilde{W}_i^T \Gamma_i^{-1} \tilde{W}_i + \sum_{i=1}^{n} \frac{1}{2}\tilde{W}_{Di}^T \Gamma_{Di}^{-1} \tilde{W}_{Di} \\ + \sum_{i=1}^{2}\sum_{j=1}^{2} \frac{1}{2}\tilde{K}_{ij}\rho_i \tilde{K}_{ij} + \frac{1}{2}\tilde{d}^T \tilde{d} \end{aligned} \tag{50}$$

where $\tilde{K}_{ij} = \hat{K}_{ij} - K_{ij}$ denotes the approximation error. Similar to (33), taking the time derivative of V_5 yields

$$\dot{V}_5 \le -c_3 V_5 + c_5 \tag{51}$$

where c_3 is the same as before and c_5 is a positive constant given as

$$\begin{aligned} c_5 = &\sum_{i=1}^{2}\sum_{j=1}^{2} \frac{\gamma_i}{2} K_{ij}\rho_i K_{ij} + \sum_{i=1}^{n} \frac{1}{2} W_{Di}^{*T} \sigma_{Di} W_{Di}^{*} \\ &+ \sum_{i=1}^{n} \frac{1}{2} W_i^{*T} \sigma_i W_i^{*} + \frac{1}{2}\bar{d}^T (I + \beta k_d)\bar{d} \\ &+ \frac{1}{2}\bar{\epsilon}_D^T (Z_D)(2\beta k_d + k_a^2)\bar{\epsilon}_D(Z_D) \\ &+ \frac{1}{2}\bar{\epsilon}^T (Z)\bar{\epsilon}(Z) + \frac{1}{2} n_D \parallel k_a W_d^* \parallel^2 \end{aligned} \tag{52}$$

Theorem 2: Similar to case A, for the robotic system considering the TLOE of actuators (41), with bounded initial conditions, SGUB stability is obtained with the DO constructed as (49) and α designed as (31). The prescribed performance of the tracking error is guaranteed, namely $\forall t > 0$, $\underline{k}_i(t) < e_i(t) < \overline{k}_i(t)$.

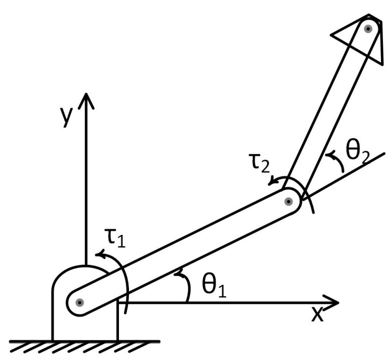

Fig. 2. A two-link planar manipulator

IV. Simulation Study

Consider a rigid robot with a uniform mass distribution shown in Fig. 2. Assumed to move on the Cartesian space, the joint variables vector q of the robot is given as

$$q = \begin{bmatrix} \theta_1 \\ \theta_2 \end{bmatrix} = \begin{bmatrix} q_1 \\ q_2 \end{bmatrix} \tag{53}$$

Then the $M(q), C(q,\dot{q}), G(q)$ in the dynamics model can be similarly obtained as in [79]. Parameters of the robot are given as

$$m_1 = 1\text{kg}, m_2 = 0.85\text{kg}, l_1 = 0.3\text{m}, l_2 = 0.4\text{m} \tag{54}$$

The desired trajectory is set as $\theta_1 = \sin(t), \theta_2 = \cos(2t)$, the states are initialized at $\theta_1(0) = 1, \theta_2(0) = 0, \dot{\theta}_1(0) = \dot{\theta}_2(0) = 0$, and the initial configuration of the neural network weight is 0. The disturbance is given as $d(t) = [\sin(t) + 1; 2\cos(t) + 0.5]^T$. For the prescribed performance, the steady state error of q_1 demands to be no more than 0.1, and the minimum convergence rate is determined by the exponential e^{-t}, and to ensure the initial error is in the bounds, ρ_0 and σ are set as $\rho_0 = 1.5, \sigma = 0.5$. Then, the performance function of q_1 is designed as $\rho(t) = (1.5 - 0.1)e^{-t} + 0.1$ The prescribed performance function of q_2 is set symmetry with q_1's. Thus, the prescribed bounds of q can be written as

$$\overline{k}(t) = \begin{bmatrix} 1.4e^{-t} + 0.1 \\ 0.7e^{-t} + 0.05 \end{bmatrix}, \underline{k}(t) = \begin{bmatrix} -0.7e^{-t} - 0.05 \\ -1.4e^{-t} - 0.1 \end{bmatrix} \tag{55}$$

The simulation study encompasses three cases, and the controller in the last case is used for comparison to show the advancement of the former two controllers. To enhance the comparability and convincingness, the design parameters of the three controllers are the same and shown in Table. 1, where η^2 is the variance of centers.

TABLE I
The design parameters

Item	K_1	K_2	$\sigma_1(\sigma_{d1}, \sigma_{D1})$	$\sigma_2(\sigma_{d2}, \sigma_{D2})$
Value	$3I_{2\times 2}$	$10I_{2\times 2}$	2	2
Item	η^2	$l(l')$	$\Gamma_1(\Gamma_{d1}, \Gamma_{D1})$	$\Gamma_2(\Gamma_{d2}, \Gamma_{D2})$
Value	1	64	$10I_{64\times 64}$	$10I_{64\times 64}$

Case 1: Controller against PLOE type of failure.

In the simulation, the failure is assumed to occur twice at $t = 1s$ and $t = 7s$, and the control torque coefficient K_t is written as

$$K_t = \begin{cases} \begin{bmatrix} 1 & 0 \\ 0 & 1 \end{bmatrix}, 0 \le t < 1 \\ \begin{bmatrix} 0.7 & 0 \\ 0 & 0.5 \end{bmatrix}, 1 \le t < 7 \\ \begin{bmatrix} 0.5 & 0 \\ 0 & 0.4 \end{bmatrix}, t \ge 7 \end{cases} \tag{56}$$

Simulation results given in Figs. 3-5 show that the desired trajectory of the joint position q is well tracked, and the tracking error e strictly remains within the prescribed bounds. From Fig. 5, it can be known that the actual input torques and the commanded torques satisfy $\tau = K_t\tau_c$.

Case 2: Controller against TLOE type of failure.

As mentioned before, when TLOE type of failure occurs to the robotic system, redundancy control technique is used. Under this circumstance, every joint has two actuators correspondingly. It is assumed that the actuator τ_1 loses effectiveness twice at $t = 1s$ and $t = 7s$, and the actuator τ_2 is stuck at $[5, 7]^T$. The parameters $\rho_1, \rho_2, \bar{\tau}_{c1}, \bar{\tau}_{c2}$ in (41) are written as

$$\rho_2 = \begin{cases} \begin{bmatrix} 1 & 0 \\ 0 & 1 \end{bmatrix}, 0 \le t < 1 \\ \begin{bmatrix} 0 & 0 \\ 0 & 0 \end{bmatrix}, t \ge 1 \end{cases} \tag{57}$$

$$\rho_1 = K_t, \bar{\tau}_{c1} = [0, 0]^T, \bar{\tau}_{c2} = [5, 7]^T \tag{58}$$

Figs. 6-8 show the simulation results. The tracking performance and the error are respectively plotted in Fig. 6 and Fig. 7, from which it can be seen that even one of the two actuators is stuck, the output can still follow the desired trajectory well and the prescribed performance is guaranteed. Fig. 8 gives the control input, where the red solid line represents the commanded torque τ_{c1}, the blue dashed line represents the actual torque generated by the actuator τ_1 which is not stuck, the green plus sign line indicates the output torque of the stuck actuator τ_2, the black dash-dotted line indicates the total torque delivered to the joint. These variables meet the setting of ρ_1 and ρ_2 expressed by (58) and (57).

Case 3: neural controller without consideration of the actuator failure and the prescribed performance

In this case, the state feedback neural controller presented in [79] is used, which doesn't take the actuator failure and the prescribed performance into consideration. Simulation results are given in Fig. 9 and Fig. 10 from which a bad tracking performance and a violation of the prescribed bounds can be found. Comparison of these simulation results in the three cases proves the advancement of our controllers.

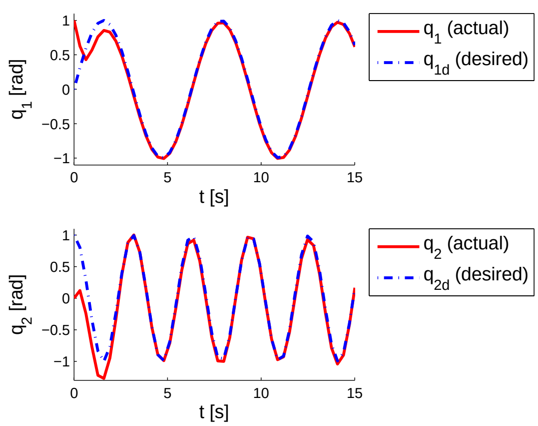

Fig. 3. Tracking performance in Case 1.

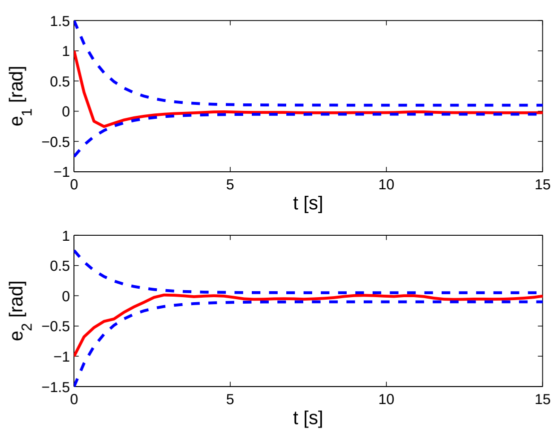

Fig. 4. Tracking errors and the prescribed bounds in Case 1.

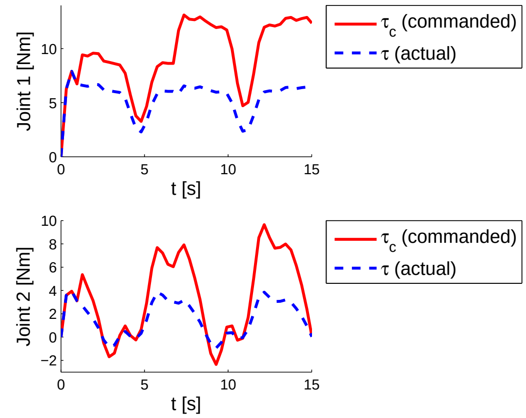

Fig. 5. Control inputs in Case 1.

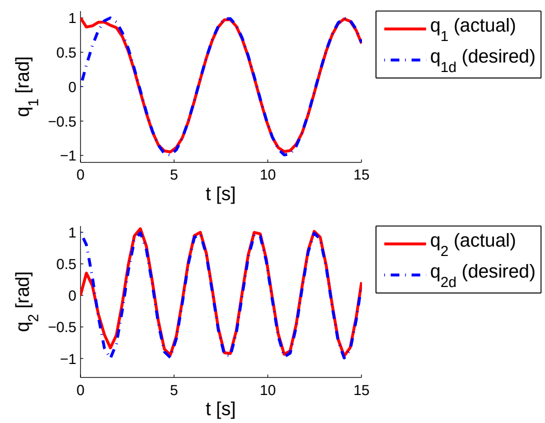

Fig. 6. Tracking performance in Case 2.

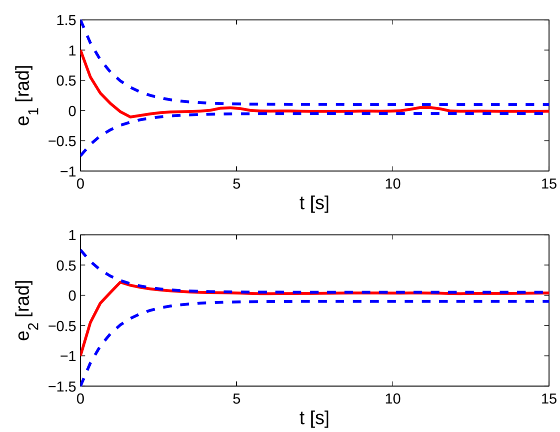

Fig. 7. Tracking errors and the prescribed bounds in Case 2.

V. Experiment

To further prove the validity of our proposed control method, we test our controller against PLOE type of failure on the Baxter robot as shown in Fig. 11. Each Baxter's joint is actuated by only one motor, so the redundant controller against TLOE which means at least two actuators at each joint cannot be implemented. The disturbances in the experiment derive

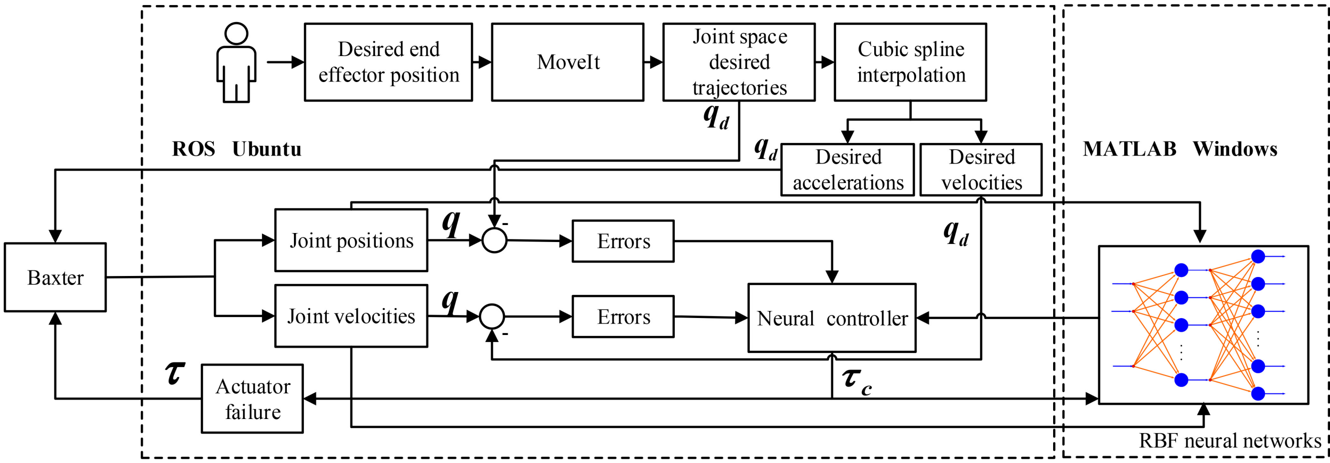

Fig. 13. The control block diagram.

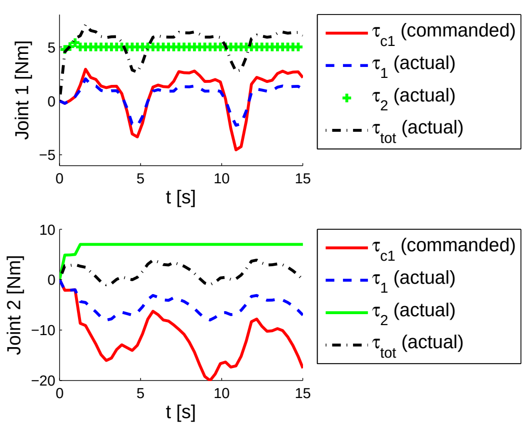

Fig. 8. Control inputs in Case 2.

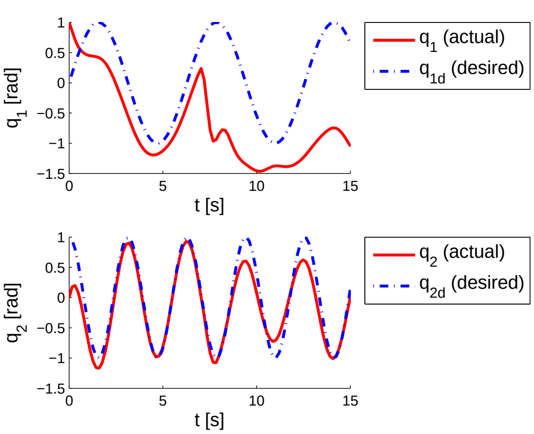

Fig. 9. Tracking performance in Case 3.

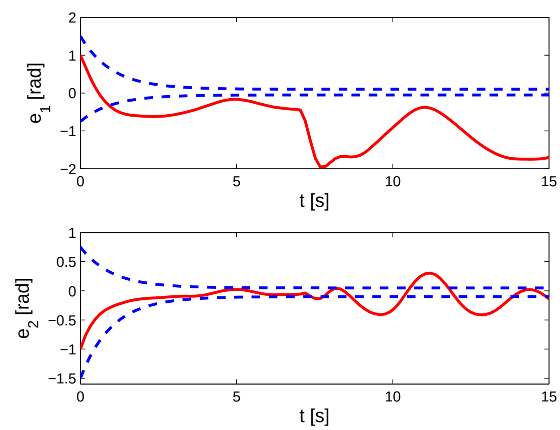

Fig. 10. Tracking errors and the prescribed bounds in Case 3.

from sensor measurement errors and communication delays. Dominated by the computing speed, we use two collaborative computers in our experiment. A slave computer with Windows operating system is used for iterative calculation of the neural networks output, and a master computer with Ubuntu operating system is applied for trajectory planning and giving the control signal to the Baxter as well as the neural input signals to the slave computer. The two computers communicate with each other through the Ethernet as shown in the experimental schematic diagram Fig. 12. The transmitting and receiving frequency of the master computer is set as 200Hz. The frequency of total closed-loop is set as 250Hz. As shown in the control block diagram Fig. 13, we input a desired position of the end effector through the master computer, then MoveIt, a state of the art software for mobile manipulation, is used for trajectory planning, and we use the cubic spline interpolation to get the velocity and acceleration expectations of the joints. Based on the neural networks output and the state feedback signals, the master computer calculate the commanded control torque τ_c. Then through the actuator failure part we designed, the motors generate actual torque τ to drive the Baxter's joints.

For simplification, the prescribed tracking error performance

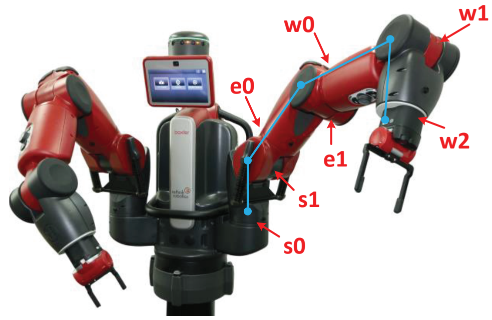

Fig. 11. The Baxter robot with seven joints.

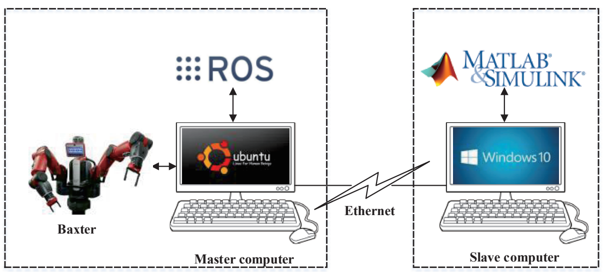

Fig. 12. The Experimental schematic diagram. The master computer with Ubuntu operating system directly generates the control command to drive the Baxter joint motors. The slave computer with Windows operating system receives the neural input from the master computer and returns the neural network output back through MATLAB.

functions for the seven joints are the same one with the upper bound set as $\rho(t) = 0.5e^{-2t} + 0.05$ and the lower bound set as $\rho(t) = -0.6e^{-2t} - 0.06$. The PLOE type of failure occurs at $t = 0.5s$ with the $K_t = 0.1I_{7\times7}$. The experiment results are given in Figs. 14-15. The angle tracking performance of the seven joints is indicated in Fig. 14 from which we can see that the errors are quickly getting small and successfully guaranteed within the prescribed bounds. Fig. 15 shows the actual torques delivered to the seven joints. A comparative PD controller is also tested on the Baxter, and Figs. 16 and 17 show the tracking performance and the actual torques, respectively. The tracking errors converge slowly with a violation of the prescribed bounds.

VI. Conclusion

Two adaptive neural control schemes have been proposed for robotic systems against PLOE and TLOE types of actuator failure, respectively. A novel DO combined with RBF neural networks is constructed to attenuate the influence of the unknown disturbance. Simulation studies show that the control method can guarantee a prescribed performance even facing with system uncertainties, unknown disturbance and actuator failure simultaneously. Moreover, implementation on a seven-joints robot gives a experimental verification of our control algorithm. However, the proposed control schemes are based on some assumptions such as finite number of failures and bounded disturbance. our future work will focus on the relaxation of these assumptions.

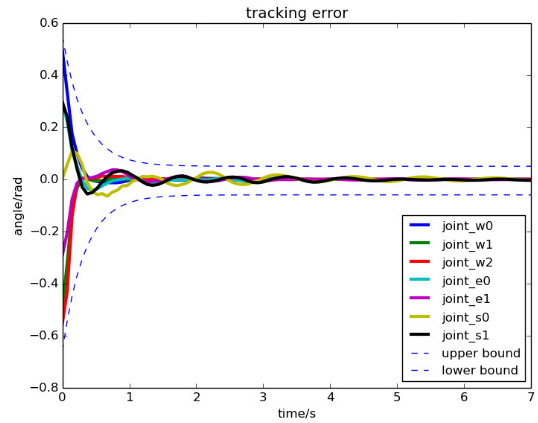

Fig. 14. The tracking errors of seven joints and their prescribed bounds under neural controller.

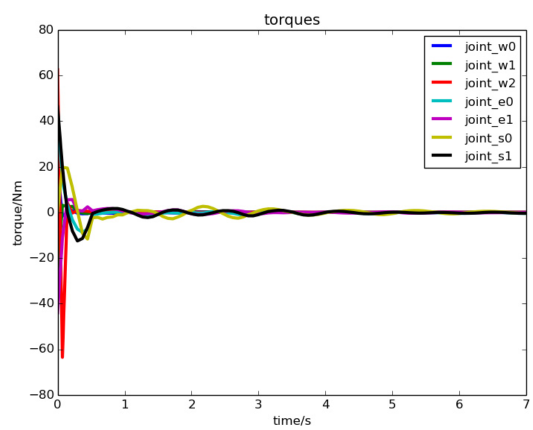

Fig. 15. The actual torques under neural controller.

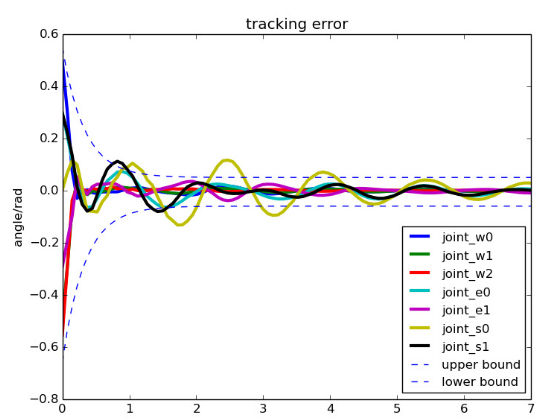

Fig. 16. The tracking errors of seven joints and their prescribed bounds under PD controller.

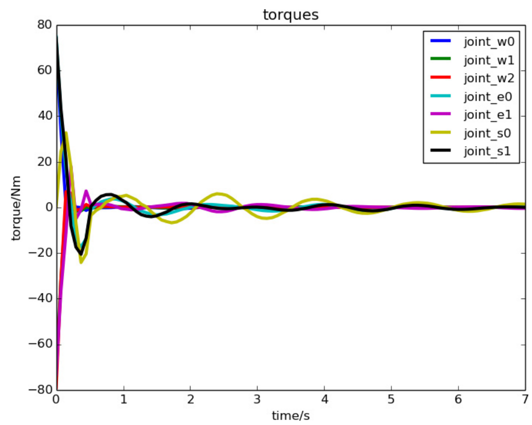

Fig. 17. The actual torques under PD controller.

REFERENCES

[1] P. Huang, F. Zhang, J. Cai, D. Wang, Z. Meng, and J. Guo, "Dexterous tethered space robot: Design, measurement, control, and experiment," *IEEE Transactions on Aerospace and Electronic Systems*, vol. 53, no. 3, pp. 1452–1468, 2017.

[2] H. Wang, R. Zhang, W. Chen, X. Liang, and R. Pfeifer, "Shape detection algorithm for soft manipulator based on fiber bragg gratings," *IEEE/ASME Transactions on Mechatronics*, vol. 21, no. 6, pp. 2977–2982, 2016.

[3] F. Zhang and P. Huang, "Releasing dynamics and stability control of maneuverable tethered space net," *IEEE/ASME Transactions on Mechatronics*, vol. 22, no. 2, pp. 983–993, 2017.

[4] H. Wang, C. Wang, W. Chen, X. Liang, and Y. Liu, "Three-dimensional dynamics for cable-driven soft manipulator," *IEEE/ASME Transactions on Mechatronics*, vol. 22, no. 1, pp. 18–28, 2017.

[5] H. Qiao, M. Wang, J. Su, S. Jia, and R. Li, "The concept of attractive region in environment and its application in high-precision tasks with low-precision systems," *IEEE/ASME Transactions on Mechatronics*, vol. 20, no. 5, pp. 2311–2327, 2015.

[6] W. He, W. Ge, Y. Li, Y. J. Liu, C. Yang, and C. Sun, "Model identification and control design for a humanoid robot," *IEEE Transactions on Systems, Man, and Cybernetics: Systems*, vol. 47, no. 1, pp. 45–57, 2017.

[7] Z. Li, B. Huang, A. Ajoudani, C. Yang, C. Y. Su, and A. Bicchi, "Asymmetric bimanual control of dual-arm exoskeletons for human-cooperative manipulations," *IEEE Transactions on Robotics*, vol. 34, no. 1, pp. 264–271, 2018.

[8] Z. Li, H. Bo, Z. Ye, M. Deng, and C. Yang, "Physical human-robot interaction of a robotic exoskeleton by admittance control," *IEEE Transactions on Industrial Electronics*, vol. 65, no. 12, pp. 9614–9624, 2018.

[9] Q. Shi, K. Li, C. Li, Q. Huang, H. Ishii, A. Takanishiand, and T. Fukuda, "A modified robotic rat to study rat-like pitch and yaw movements," *IEEE/ASME Transactions on Mechatronics*, vol. 23, no. 5, pp. 2448–2458, 2018.

[10] Z. Gao, Q. Shi, T. Fukuda, C. Li, and Q. Huang, "An overview of biomimetic robots with animal behaviors," *Neurocomputing*, vol. 332, pp. 339–350, 2019.

[11] W. He, Z. Li, and C. P. Chen, "A survey of human-centered intelligent robots: issues and challenges," *IEEE/CAA Journal of Automatica Sinica*, vol. 4, no. 4, pp. 602–609, 2017.

[12] J. D. Boskovic and R. K. Mehra, "Multiple-model adaptive flight control scheme for accommodation of actuator failures," *Journal of Guidance Control & Dynamics*, vol. 25, no. 4, pp. 712–724, 2002.

[13] J. Jiang, "Design of reconfigurable control systems using eigenstructure assignments," *International Journal of Control*, vol. 59, no. 2, pp. 395–410, 2011.

[14] M. L. Corradini and G. Orlando, "Actuator failure identification and compensation through sliding modes," *IEEE Transactions on Control Systems Technology*, vol. 15, no. 1, pp. 184–190, 2006.

[15] J. Li, X. Li, and Q. Su, "Fault detection filter design for discrete-time switched time-delay systems with static quantizer and quantized feedback," *International Journal of Innovative Computing, Information and Control*, vol. 14, no. 4, pp. 1465–1479, 2018.

[16] M. Gao, S. Jiang, and F. Pan, "Fault detection for time-delayed networked control systems with sensor saturation and randomly occurring faults," *International Journal of Innovative Computing, Information and Control*, vol. 14, no. 4, pp. 1511–1525, 2018.

[17] X. Liu, X. Su, P. Shi, S. K. Nguang, and C. Shen, "Fault detection filtering of nonlinear switched systems via event-triggered communication approach," *Automatica*, vol. 101, pp. 365–376, 2019.

[18] X. Su, F. Xia, L. Wu, and C. L. P. Chen, "Event-triggered fault detector and controller coordinated design of fuzzy systems," *IEEE Transactions on Fuzzy Systems*, vol. 26, no. 4, pp. 2004–2016, 2018.

[19] X. Tang, G. Tao, and S. M. Joshi, "Adaptive actuator failure compensation for nonlinear mimo systems with an aircraft application," *Automatica*, vol. 43, no. 11, pp. 1869–1883, 2007.

[20] J. Peng, X. Fu, and Y. Chen, "Response of a swirlmeter to oscillatory flow," *Flow Measurement and Instrumentation*, vol. 19, no. 2, pp. 107–115, 2008.

[21] J. Peng, X. Fu, and Y. Chen, "Experimental investigations of strouhal number for flows past dual triangulate bluff bodies," *Flow Measurement and Instrumentation*, vol. 19, no. 6, pp. 350–357, 2008.

[22] Y. Song and X. Yuan, "Low-cost adaptive fault-tolerant approach for semiactive suspension control of high-speed trains," *IEEE Transactions on Industrial Electronics*, vol. 63, no. 11, pp. 7084–7093, 2016.

[23] X. Su, X. Liu, and Y. Song, "Fault-tolerant control of multi-area power systems via sliding mode observer technique," *IEEE/ASME Transactions on Mechatronics*, vol. 23, no. 1, pp. 38 – 47, 2017.

[24] L. Wang, M. Basin, H. Li, and R. Lu, "Observer-based composite adaptive fuzzy control for nonstrict-feedback systems with actuator failures," *IEEE Transactions on Fuzzy Systems*, vol. 26, no. 4, pp. 2336 – 2347, 2018.

[25] Y. Guo, B. Jiang, and Y. Zhang, "A novel robust attitude control for quadrotor aircraft subject to actuator faults and wind gusts," *IEEE/CAA Journal of Automatica Sinica*, vol. 5, no. 1, pp. 292–300, 2018.

[26] P. Huang, D. Wang, F. Zhang, Z. Meng, and Z. Liu, "Postcapture robust nonlinear control for tethered space robot with constraints on actuator and velocity of space tether," *International Journal of Robust & Nonlinear Control*, vol. 27, no. 16, pp. 2824–2841, 2017.

[27] Y. Zhang, H. Li, J. Sun, and W. He, "Cooperative adaptive event-triggered control for multi-agent systems with actuator failures," *IEEE Transactions on Systems, Man and Cybernetics: Systems*, 2018, In Press, DOI: 10.1109/TSMC.2018.2883907.

[28] G. Bingwei and H. Wenlong, "Neural network model reference decoupling control for single leg joint of hydraulic quadruped robot," *Assembly Automation*, vol. 38, no. 4, pp. 465–475, 2018.

[29] L. Pan, G. Bao, F. Xu, and L. Zhang, "Adaptive robust sliding mode trajectory tracking control for 6 degree-of-freedom industrial assembly robot with disturbances," *Assembly Automation*, vol. 38, no. 3, pp. 259–267, 2018.

[30] H. Chen, L. Chen, Q. Zhang, and F. Tong, "Visual servoing of dynamic wheeled mobile robots with anti-interference finite-time controllers," *Assembly Automation*, vol. 38, no. 5, pp. 558–567, 2018.

[31] Q. C. Nguyen, M. Piao, and K.-S. Hong, "Multivariable adaptive control of the rewinding process of a roll-to-roll system governed by hyperbolic partial differential equations," *International Journal of Control, Automation and Systems*, vol. 16, no. 5, pp. 2177–2186, 2018.

[32] K. D. Kallu, W. Jie, and M. C. Lee, "Sensorless reaction force estimation of the end effector of a dual-arm robot manipulator using sliding mode control with a sliding perturbation observer," *International Journal of Control, Automation and Systems*, vol. 16, no. 3, pp. 1367–1378, 2018.

[33] X. Chen, Y. Feng, and C.-Y. Su, "Adaptive control for continuous-time systems with actuator and sensor hysteresis," *Automatica*, vol. 64, pp. 196–207, 2016.

[34] X. Chen, C.-Y. Su, Z. Li, and F. Yang, "Design of implementable adaptive control for micro/nano positioning system driven by piezoelectric actuator," *IEEE Transactions on Industrial Electronics*, vol. 63, no. 10, pp. 6471–6481, 2016.

[35] M. Bergerman and Y. S. Xu, "Robust joint and cartesian control of underactuated manipulators," *Journal of Dynamic Systems Measurement & Control*, vol. 118, no. 3, pp. 557–565, 1996.

[36] J.-H. Shin and W.-H. Kim, "Robust adaptive neural control for a robotic system with performance degradation of actuators," in *2006 SICE-ICASE International Joint Conference*. IEEE, 2006, pp. 2993–2998.

[37] H. Qiao, J. Peng, Z.-B. Xu, and B. Zhang, "A reference model approach to stability analysis of neural networks," *IEEE Transactions on Systems, Man, and Cybernetics, Part B (Cybernetics)*, vol. 33, no. 6, pp. 925–936, 2003.

[38] D. Wang, D. Liu, H. Li, B. Luo, and H. Ma, "An approximate optimal control approach for robust stabilization of a class of discrete-time

nonlinear systems with uncertainties," *IEEE Transactions on Systems, Man, & Cybernetics Systems*, vol. 46, no. 5, pp. 713–717, 2015.

[39] Y. Song, X. Huang, and C. Wen, "Tracking control for a class of unknown nonsquare mimo nonaffine systems: A deep-rooted information based robust adaptive approach," *IEEE Transactions on Automatic Control*, vol. 61, no. 10, pp. 3227–3233, 2016.

[40] D. Wang, H. He, and D. Liu, "Improving the critic learning for event-based nonlinear H_∞ control design," *IEEE Transactions on Cybernetics*, vol. 47, no. 10, pp. 3417–3428, 2017.

[41] Q. Guo, Y. Zhang, B. G. Celler, and S. W. Su, "Backstepping control of electro-hydraulic system based on extended-state-observer with plant dynamics largely unknown," *IEEE Transactions on Industrial Electronics*, vol. 63, no. 11, pp. 6909–6920, 2016.

[42] H. Yang and J. Liu, "An adaptive rbf neural network control method for a class of nonlinear systems," *IEEE/CAA Journal of Automatica Sinica*, vol. 5, no. 2, pp. 457–462, 2018.

[43] J. Wei, Y. A. Hu, and M. Sun, "An exploration on adaptive iterative learning control for a class of commensurate high-order uncertain nonlinear fractional order systems," *IEEE/CAA Journal of Automatica Sinica*, vol. 4, no. 2, pp. 618 – 627, 2018.

[44] L. Xue, C. Sun, D. Wunsch, Y. Zhou, and F. Yu, "An adaptive strategy via reinforcement learning for the prisoner's dilemma game," *IEEE/CAA Journal of Automatica Sinica*, vol. 5, no. 1, pp. 301 – 310, 2018.

[45] Y. Kang, D.-H. Zhai, G.-P. Liu, Y.-B. Zhao, and P. Zhao, "Stability analysis of a class of hybrid stochastic retarded systems under asynchronous switching," *IEEE Transactions on Automatic Control*, vol. 59, no. 6, pp. 1511–1523, 2014.

[46] Y. Kang, D.-H. Zhai, G.-P. Liu, and Y.-B. Zhao, "On input-to-state stability of switched stochastic nonlinear systems under extended asynchronous switching," *IEEE Transactions on Cybernetics*, vol. 46, no. 5, pp. 1092–1105, 2016.

[47] X. Su, Y. Wen, Y. D. Song, and T. Hayat, "Dissipativity-based fuzzy control of nonlinear systems via an event-triggered mechanism," *IEEE Transactions on Systems, Man,and Cybernetics: Systems*, 2018, In Press, DOI: 10.1109/TSMC.2017.2713420.

[48] X. Su, P. Shi, L. Wu, and M. V. Basin, "Reliable filtering with strict dissipativity for t-s fuzzy time-delay systems." *IEEE Transactions on Cybernetics*, vol. 44, no. 12, pp. 2470–2483, 2017.

[49] G. Wu, J. Sun, and J. Chen, "Optimal linear quadratic regulator of switched systems," *IEEE Transactions on Automatic Control*, 2018, In Press, DOI 10.1109/TAC.2018.2872204.

[50] Z. Tong, C. L. P. Chen, C. Long, X. Xu, and B. Hu, "Design of highly nonlinear substitution boxes based on i-ching operators," *IEEE Transactions on Cybernetics*.

[51] C. L. Chen, T. Zhang, L. Chen, and S. C. Tam, "I-ching divination evolutionary algorithm and its convergence analysis," *IEEE Transactions on Cybernetics*, vol. 47, no. 1, pp. 2–13, 2017.

[52] S. Jung, "Improvement of tracking control of a sliding mode controller for robot manipulators by a neural network," *International Journal of Control, Automation and Systems*, vol. 16, no. 2, pp. 937–943, 2018.

[53] F. Zouari, A. Ibeas, A. Boulkroune, J. Cao, and M. M. Arefi, "Adaptive neural output-feedback control for nonstrict-feedback time-delay fractional-order systems with output constraints and actuator nonlinearities," *Neural Networks*, vol. 105, pp. 256–276, 2018.

[54] B. Xu, "Composite learning finite-time control with application to quadrotors," *IEEE Transactions on Systems, Man, and Cybernetics: Systems*, vol. 48, no. 10, pp. 1806–1815, 2018.

[55] W. He and S. S. Ge, "Vibration control of a nonuniform wind turbine tower via disturbance observer," *IEEE/ASME Transactions on Mechatronics*, vol. 20, no. 1, pp. 237–244, 2014.

[56] M. Chen, P. Shi, and C. C. Lim, "Robust constrained control for mimo nonlinear systems based on disturbance observer," *IEEE Transactions on Automatic Control*, vol. 60, no. 12, pp. 3281–3286, 2015.

[57] M. Chen, S. Y. Shao, P. Shi, and Y. Shi, "Disturbance observer based robust synchronization control for a class of fractional-order chaotic systems," *IEEE Transactions on Circuits & Systems II Express Briefs*, vol. 64, no. 4, pp. 417–421, 2017.

[58] B. Xu, "Composite learning control of flexible-link manipulator using nn and dob," *IEEE Transactions on Systems, Man, and Cybernetics: Systems*, vol. 48, no. 11, pp. 1979–1985, 2018.

[59] M. Chen, P. Shi, and C. C. Lim, "Adaptive neural fault-tolerant control of a 3-dof model helicopter system," *IEEE Transactions on Systems, Man, and Cybernetics: Systems*, vol. 46, no. 2, pp. 260–270, 2016.

[60] M. Chen and S. S. Ge, "Adaptive neural output feedback control of uncertain nonlinear systems with unknown hysteresis using disturbance observer," *IEEE Transactions on Industrial Electronics*, vol. 62, no. 12, pp. 7706–7716, 2015.

[61] S.-L. Dai, C. Wang, and M. Wang, "Dynamic learning from adaptive neural network control of a class of nonaffine nonlinear systems," *IEEE Transactions on Neural Networks & Learning Systems*, vol. 25, no. 1, pp. 111–123, 2014.

[62] S.-L. Dai, S. He, M. Wang, and C. Yuan, "Adaptive neural control of underactuated surface vessels with prescribed performance guarantees," *IEEE Transactions on Neural Networks & Learning Systems*, 2018, In Press, DOI: 10.1109/TNNLS.2018.2876685.

[63] S.-L. Dai, S. He, H. Lin, and C. Wang, "Platoon formation control with prescribed performance guarantees for usvs," *IEEE Transactions on Industrial Electronics*, vol. 65, no. 5, pp. 4237–4246, 2018.

[64] S.-L. Dai, M. Wang, and C. Wang, "Neural learning control of marine surface vessels with guaranteed transient tracking performance," *IEEE Transactions on Industrial Electronics*, vol. 63, no. 3, pp. 1717–1727, 2016.

[65] H. Xu and P. A. Ioannou, "Robust adaptive control for a class of mimo nonlinear systems with guaranteed error bounds," *IEEE Transactions on Automatic Control*, vol. 48, no. 5, pp. 728–742, 2002.

[66] J. Zhou, C. Wen, and Y. Zhang, "Adaptive backstepping control of a class of uncertain nonlinear systems with unknown backlash-like hysteresis," *IEEE Transactions on Automatic Control*, vol. 49, no. 10, pp. 1751–1759, 2004.

[67] K. P. Tee, S. S. Ge, and E. H. Tay, "Barrier lyapunov functions for the control of output-constrained nonlinear systems," *Automatica*, vol. 45, no. 4, pp. 918–927, 2009.

[68] B. Xu, Z. Shi, F. Sun, and W. He, "Barrier lyapunov function based learning control of hypersonic flight vehicle with AOA constraint and actuator faults," *IEEE Transactions on Cybernetics*, vol. 49, no. 3, pp. 1047 – 1057, 2019.

[69] S. Zhang, Y. Dong, Y. Ouyang, Z. Yin, and K. Peng, "Adaptive neural control for robotic manipulators with output constraints and uncertainties," *IEEE Transactions on Neural Networks & Learning Systems*, vol. 29, no. 11, pp. 5554 – 5564, 2018.

[70] H. Li, S. Zhao, W. He, and R. Lu, "Adaptive finite-time tracking control of full states constrained nonlinear systems with dead-zone," *Automatica*, vol. 100, pp. 99–107, 2019.

[71] C. P. Bechlioulis and G. A. Rovithakis, "Robust adaptive control of feedback linearizable mimo nonlinear systems with prescribed performance," *IEEE Transactions on Automatic Control*, vol. 53, no. 9, pp. 2090–2099, 2008.

[72] W. Wang and C. Wen, "Adaptive actuator failure compensation control of uncertain nonlinear systems with guaranteed transient performance," *Automatica*, vol. 46, no. 12, pp. 2082–2091, 2010.

[73] L. Zhang, Y. Li, and S. Tong, "Adaptive fuzzy output feedback control for mimo switched nonlinear systems with prescribed performances," *Fuzzy Sets & Systems*, vol. 306, pp. 153–168, 2015.

[74] W. Shi and B. Li, "Adaptive fuzzy control for feedback linearizable mimo nonlinear systems with prescribed performance," *Fuzzy Sets & Systems*, vol. 344, pp. 70–89, 2018.

[75] Q. Zhou, H. Li, L. Wang, and R. Lu, "Prescribed performance observer-based adaptive fuzzy control for nonstrict-feedback stochastic nonlinear systems," *IEEE Transactions on Systems, Man, anf Cybernetics: Systems*, vol. 48, no. 10, pp. 1747 – 1758, 2018.

[76] C. Yang, X. Wang, L. Cheng, and H. Ma, "Neural-learning-based telerobot control with guaranteed performance," *IEEE Transactions on Cybernetics*, vol. 47, no. 10, pp. 3148–3159, 2017.

[77] W. He, H. Huang, and S. S. Ge, "Adaptive neural network control of a robotic manipulator with time-varying output constraints," *IEEE Transactions on Cybernetics*, vol. 47, no. 10, pp. 3136–3147, 2017.

[78] G. Antonelli, "Stability analysis for prioritized closed-loop inverse kinematic algorithms for redundant robotic systems," *IEEE Transactions on Robotics*, vol. 25, no. 5, pp. 985–994, 2009.

[79] W. He, S. S. Ge, Y. Li, E. Chew, and Y. S. Ng, "Neural network control of a rehabilitation robot by state and output feedback," *Journal of Intelligent & Robotic Systems*, vol. 80, no. 1, pp. 15–31, 2015.

Haifeng Huang (S'16) received the B.Eng. degree in automation from the School of Automation and Electrical Engineering, University of Science and Technology Beijing, Beijing, China, in 2016, where he is currently pursuing the Ph.D. degree.

His current research interests include bionic flapping-wing robot, neural network control and fault-tolerant control.

Wei He (S'09-M'12-SM'16) received his B.Eng. in automation and his M.Eng. degrees in control science and engineering from College of Automation Science and Engineering, South China University of Technology (SCUT), China, in 2006 and 2008, respectively, and his Ph.D. degree in control science and engineering from from Department of Electrical & Computer Engineering, the National University of Singapore (NUS), Singapore, in 2011.

He is currently working as a full professor in School of Automation and Electrical Engineering, University of Science and Technology Beijing, Beijing, China. He has co-authored 2 books published in Springer and published over 100 international journal and conference papers. He was awarded a Newton Advanced Fellowship from the Royal Society, UK in 2017. He was a recipient of the IEEE SMC Society Andrew P. Sage Best Transactions Paper Award in 2017. He is serving the Chair of IEEE SMC Society Beijing Capital Region Chapter. He is serving as an Associate Editor of *IEEE Transactions on Neural Networks and Learning Systems*, *IEEE Transactions on Control Systems Technology*, *IEEE Transactions on Systems, Man, and Cybernetics: Systems*, *IEEE/CAA Journal of Automatica Sinica*, *Neurocomputing*, and an Editor of *Journal of Intelligent & Robotic Systems*.

His current research interests include robotics, distributed parameter systems and intelligent control systems.

Jiashu Li received the B.Eng. degree from the School of Automation and Electrical Engineering, University of Science and Technology Beijing, Bejing, China, in 2018, where he is currently pursuing the M.E. degree.

His current research interests include neural network control, motion planning and robotics.

Bin Xu received the B.S. degree in measurement and control from Northwestern Polytechnical University, China, 2006 and the Ph.D. degree in Computer Science from Tsinghua University, China, 2012. He is currently professor with School of Automation, Northwestern Polytechnical University. His research interests include intelligent control and adaptive control with application to flight dynamics. Dr. Xu is an Associate Editor of *Neurocomputing* and *IEEE Access*.

Chenguang Yang (M'10-SM'16) is a Professor of Robotics. He received the B.Eng. degree in measurement and control from Northwestern Polytechnical University, Xi'an, China, in 2005, and the Ph.D. degree in control engineering from the National University of Singapore, Singapore, in 2010. He received postdoctoral training at Imperial College London, UK, from 2009 to 2010. He was awarded Marie Curie International Incoming Fellowship, EPSRC Innovation Fellowship, and the Best Paper Award of the IEEE Transactions on Robotics as well as over ten conference Best Paper Awards.

His research interest lies in human robot interaction and intelligent system design.

Weicun Zhang is an associate professor at the School of Automation and Electrical Engineering, University of Science and Technology Beijing. He obtained his Ph.D. degree in control theory and applications from Tsinghua University in 1993. His research interest covers adaptive control, multiple model adaptive control, intelligent control, and their applications.